Title

In Situ Spatial Complementation of Aptamer-Mediated Recognition Enables Live-Cell Imaging of Native RNA Transcripts in Real Time

Journal

Angewandte Chemie, 130(4)

ISSN

0044-8249

Authors

Wang, Zejun
Luo, Yao
Xie, Xiaodong
et al.

Publication Date

2018-01-22

DOI

10.1002/ange.201707795

Peer reviewed

Angewandte
GDCh
Chemie
Eine Zeitschrift der Gesellschaft Deutscher Chemiker
www.angewandte.de

Akzeptierter Artikel

Titel: In-situ Spatial Complementation of Aptamer-mediated Recognition Enables Live-cell Imaging of Native RNA Transcripts in Real Time

Autoren: Zejun Wang, Yao Luo, Xiaodong Xie, Xingjie Hu, Haiyun Song, Yun Zhao, Jiye Shi, Lihua Wang, Gennadi Glinsky, Nan Chen, Ratnesh Lal, and Chunhai Fan

Zitierweise: *Angew. Chem. Int. Ed.* 10.1002/anie.201707795
Angew. Chem. 10.1002/ange.201707795

Link zur VoR: http://dx.doi.org/10.1002/anie.201707795
http://dx.doi.org/10.1002/ange.201707795

WILEY-VCH

10.1002/ange.201707795

WILEY-VCH

In-situ Spatial Complementation of Aptamer-mediated Recognition Enables Live-cell Imaging of Native RNA Transcripts in Real Time

Zejun Wang, Yao Luo, Xiaodong Xie, Xingjie Hu, Haiyun Song, Yun Zhao, Jiye Shi, Lihua Wang, Gennadi Glinsky, Nan Chen*, Ratnesh Lal, Chunhai Fan*

Abstract: Direct cellular imaging of the localization and dynamics of biomolecules helps to understand their functions and reveals novel mechanisms at the single-cell resolution. In contrast to routine fluorescent protein-based protein imaging, technology for RNA imaging remains less well explored due to the lack of enabling technology. Here, we report the development of an aptamer-initiated fluorescence complementation (AiFC) method for RNA imaging by engineering a green fluorescence protein (GFP)-mimicking turn-on RNA aptamer, Broccoli, into two split fragments that could tandemly bind to target mRNA. When genetically encoded in cells, endogenous mRNA molecules recruited Split-Broccoli and brought the two fragments to the spatial proximity, which in-situ formed a fluorophore-binding site and turned on fluorescence. Significantly, we demonstrated the use of AiFC for high-contrast and real-time imaging of endogenous RNA molecules in living mammalian cells. We envision wide application and practical utility of this enabling technology to in vivo single-cell visualization and mechanistic analysis of macromolecular interactions.

Visualization of the distribution and dynamics of RNA provides key knowledge about RNA localization and trafficking in cells, which play important roles in gene expression and regulation.[1] Since RNA is inherently non-fluorescent at visible wavelengths, RNA fluorescence in situ hybridization (FISH) was developed in the 1980s to image RNAs in fixed cells.[2] To realize live-cell imaging that provides dynamic information of intracellular RNA, researchers developed various ways to engineer RNA transcripts.[3] Singer and colleagues pioneered the use of a MS2 fluorescent reporter system for genetically encoded imaging of RNA,[4] which nevertheless requires engineering of target RNAs that may alter their abundance and translational behavior. In addition, unbound MS2 fluorescent reporters often generate high fluorescence background in the cytosol. Recently, Jaffrey and coworkers [5] proposed a spectrum of green fluorescent protein (GFP)-mimicking turn-on RNA aptamers that fluorescence in the presence of a cell-permeable fluorophore, 3,5-difluoro-4-hydroxybenzylidene imidazolinone [6] (DFHBI). Fusion of these RNA aptamers named after vegetables (e.g. Spinach, Broccoli) allows fluorescence imaging of endogenous RNAs with reduced background interference.[7]

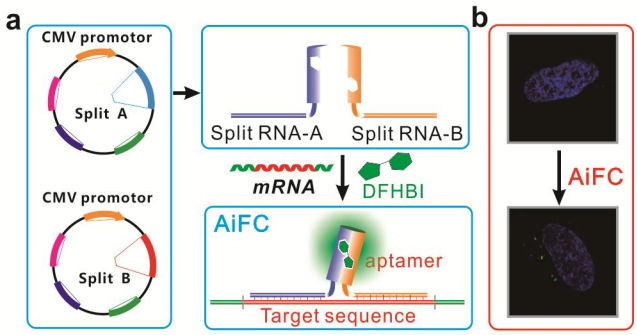

Scheme 1. (a) Design and (b) cellular expression of Broccoli-based AiFC probes for live-cell imaging of unmodified RNA transcripts.

Direct imaging of non-engineered, endogenous mRNAs remains a hurdle, although studies on native mRNAs should in principle provide unperturbed information of RNAs with better precision and quantification ability.[8] To detect a specific RNA in living cells, several groups have developed various hybridization-based turn-on fluorescent DNA/RNA probes including molecular beacons,[9] nano beacons,[10] and nano flares.[11] These probes stay in the OFF state until they hybridize to a specific region of mRNA. However, to function in cells, these probes should be micro-injected or transfected into cytosols, which is invasive and often position-specific. Here, we have developed genetically encoded probes for non-invasive imaging of unmodified endogenous RNA in living cells. Our approach was inspired by a popularly used and powerful protein imaging method for analyzing protein-protein interactions, i.e. bimolecular fluorescence complementation [12] (BiFC). In BiFC, a fluorescent protein is split into two fragments, which are fused to two different proteins of interest. Existence of specific protein-protein interactions should bring the two complementary fragments to the proximity that allows the refolding of the fluorescent protein reporter to its native conformation and emit fluorescent signal. We engineered the turn-on DFHBI-binding

[a] Z. Wang [+], X. Xie, X. Hu, Profs. L. Wang, N. Chen, C. Fan
Division of Physical Biology & Bioimaging Center
Shanghai Institute of Applied Physics, Chinese Academy of Sciences, University of Chinese Academy of Sciences
Shanghai 201800, China
E-mail: chennan@sinap.ac.cn
fchh@sinap.ac.cn
[b] Y. Luo [+], Prof. Y. Zhao
School of Life Sciences, Sichuan University
Chengdu 610064, China
[c] Prof. H. Song
Shanghai Institutes for Biological Sciences, Chinese Academy of Sciences
Shanghai 200031, China
[d] Dr. J. Shi
UCB Pharma, 208 Bath Road, Slough, SL1 3WE, UK
[e] Dr. G. Glinsky, Prof. R. Lal
University of California
San Diego, 9500 Gilman Drive, La Jolla, CA 92093, USA
[+] These authors contributed equally to this work.

Supporting information for this article is given via a link at the end of the document

RNA aptamers by splitting them to two complementary fragments, each appended with a specific recognition segment. When genetically encoded in cells, nascent mRNA transcripts recruited split aptamers and brought the two fragments to the proximity, which generated an active DFHBI-binding site that attracted DFHBI and turned on fluorescence (Scheme 1). This genetically encoded aptamer-initiated fluorescence complementation (AiFC) does not require prior modification of mRNA transcripts and can target any position of interest, which should open new avenues for RNA imaging in situ.

We first chose Baby Spinach and Broccoli as the model systems from a spectrum of GFP-mimicking RNA aptamers,[7b, 13] since they have shorter probe length (51 nt and 49 nt) and are free of undesired intramolecular structures. Previous studies suggested that the third stem loop of Spinach might be a candidate position for splitting since it shows tolerance for various modifications.[14] Hence, we chose to split Broccoli after the 22nd nucleotide (from the 5'-end) and to split Baby Spinach after the 23rd nucleotide (from the 5'-end) at the UUCG loop, which corresponded to the position of the third stem loop of Spinach. A recognition block containing 20 nt (28nt) of complementary sequence of target mRNA was split into two 10nt-long (14nt) fragments. Each pair of AiFC probes contained two Split-Broccoli (Split-Baby Spinach) sequences extended with recognition RNA sequences.

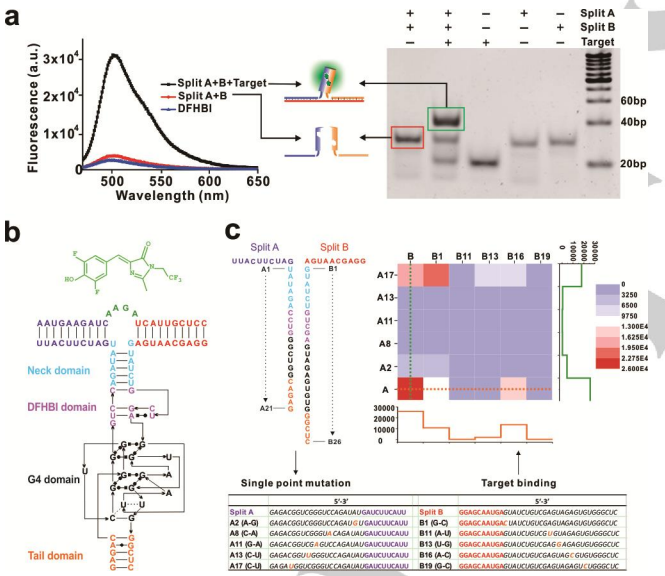

Figure 1. Fluorescence and gel analysis of AiFC probe. (a) (Left) Fluorescence intensities of Split-Broccoli (1 μM) with 10 μM DFHBI in the presence or absence of 1 μM target RNA. (Right) 8% PAGE analysis of AiFC probes with and without target RNA. Fluorescence structure (green frame) of 1 μM AiFC probe is formed in the presence of equal molar target RNA. (b) Chemical structure of DFHBI-1T and secondary structure of AiFC probe in hybridization with target RNA. (c) Heat map (right) depicting the in vitro re-association efficiency of point mutated AiFC probes listed in the table below. Mutations at DFHBI or G4 domain diminish fluorescence activation. The intensity graph at the right and bottom are corresponded to the fluorescence intensity of the vertical and horizontal dashed lines, respectively.

Next, we tested whether the two split probes could readily and stably re-associate into a functional DFHBI-binding unit in the presence of target RNA. The assembly of the two RNA probes *in vitro* was verified with polyacrylamide gel electrophoresis (PAGE), which showed that, in the presence of target RNA and DFHBI, a single band was formed with delayed migration rate, implying the formation of a complex structure. In contrast, in the absence of target RNA, the mixture of probe A and probe B migrated at the rate comparable to single probe. Thus the target RNA could effectively recruit the two split aptamer fragments into proximity (Figure. 1a). To investigate whether the two AiFC probes can reassemble into a functional conformation for DFHBI binding, we further analyzed the products with fluorescence spectroscopy. Both Split-Broccoli and Split-Baby Spinach probe pairs show little fluorescence signals without complementary RNA, even in the presence of excess DFHBI, indicating low background. DFHBI fluorescence was detected only when target RNA was added to the system. In the presence of equal molar target RNA, the fluorescence signal-to-background ratio (S/B) of Split-Broccoli and Split-Baby Spinach reached 8 and 7, respectively (Figure. 1a and Figure. S1a). We further investigated the selectivity of the AiFC probes over its target RNA. A complementary RNA sequence containing 2 nt mismatch caused a 80% loss of the fluorescence (Figure. S2), suggesting the high selectivity of AiFC. To study the correlation between fluorescence intensity and target concentrations, 500 nM AiFC probes were mixed with target RNAs of gradient concentrations from 0 nM to 500 nM, fluorescence intensity increased in a linear dose-response manner for both Split-Broccoli and Split-Baby Spinach probe pairs. (Figure. S3). In addition, although the 3D structure of Broccoli has not been determined, our results strongly suggested that Broccoli also contained a similar core structure of 3-tetrad G-quadruplex for DFHBI binding (see Figure. S4).

To further define the structural features of Broccoli, we designed a screen experiment to investigate the contribution of different regions in Broccoli AiFC probes to fluorescence activation. According to the predicted 2-D structure of Broccoli, the AiFC probe was divided into 4 main regions, namely the neck domain, DFHBI binding domain, G4 domain and tail domain (Figure. 1b). We randomly mutated 1-2 nucleotides within each domain and generated 5 mutated sequences for each probe. As a result, a total of 6×6 combination of AiFC array was formed, including the parent probe pair and 35 probe pairs bearing individual mutations (Figure. 1c). Subsequently, we measured the fluorescence intensities of 36 combinations of AiFC arrays in the presence of the target RNA and DFHBI. We found that the original design of the AiFC probe pair exhibited the brightest fluorescence signal. Point mutations within the G4 and DFHBI binding domain greatly impaired the performance of AiFC probes; whereas the neck and tail domains appeared to be more tolerant of mutations. These data provide rich information for structural configuration of Broccoli. Our results strongly suggest that conformation of G4 and fluorophore binding domains are highly conserved in these DFHBI-dependent RNA aptamers and single mutation within these regions can completely destroy RNA folding and the fluorescence. Further, assays in cell lysates revealed that Split-Baby Broccoli was fully compatible with cell studies (see Figure. S5).

Next, we examined the ability of AiFC probes for detecting endogenous mRNA in living cells. A pair of Split-Broccoli probes containing targeting sequence complementary to human β-actin mRNA were designed. Two probes were individually prepared by in vitro transcription and co-transfected into HeLa cells. The cells were then analyzed under a confocal microscope in the presence of fluorophore. DFHBI-1T, which is an improved version of DFHBI, was applied for live cell imaging (Figure. S6). Intense fluorescence signals were detected in the cytoplasm after transfection of AiFC probes; while un-transfected control cells exhibited negligible background.

In order to determine the specificity of the detected fluorescence signals for β-actin mRNAs, we introduced a Cy3-labled DNA probe that targeted β-actin mRNA but was complementary to a different sequence (Figure. 2a). Perfect co-localization of green (AiFC probes) and red (Cy3-DNA probe) signals were observed, confirming the β-actin mRNA identity of observed signals.

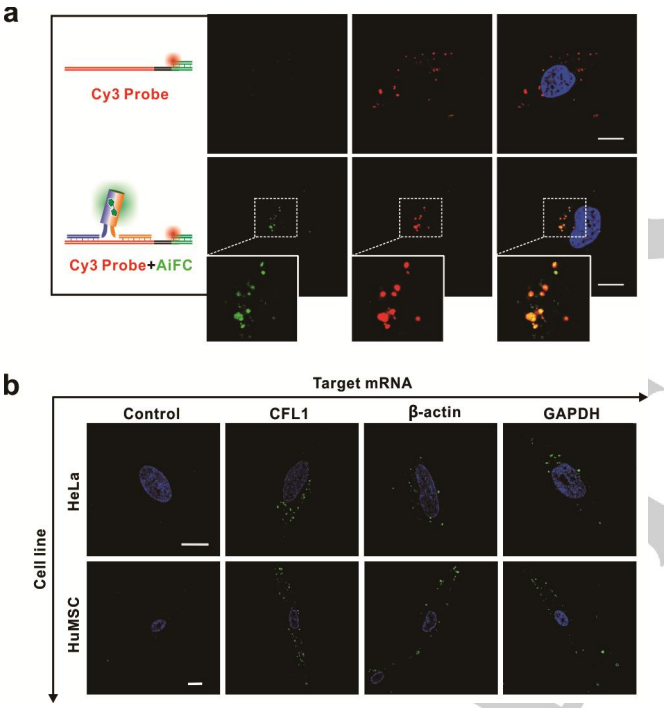

Figure 2. In vitro transcribed AiFC probes can detect native mRNA in living cells. (a) Confocal images of co-localized Cy3-DNA probe (red) and AiFC probes (green) targeting β-actin mRNA in HeLa cells. Nucleus was stained with Hoechst (Blue). (b) Visualization of the endogenous mRNAs (CFL1, β-actin, GAPDH) in HeLa cells and HuMSC cells with corresponding AiFC probes. Scale bars: 20 μm.

We next explored the general applicability of AiFC method. We replaced the recognition blocks in the Split-Broccoli probes with sequences complementary to other endogenous mRNAs including cofilin 1 (CFL1) and glyceraldehyde-3-phosphate dehydrogenase GAPDH (Table S1). Fluorescence signals were readily detected in the cytoplasm after transfection of corresponding AiFC probes, indicating the versatility of AiFC method. Encouraged by the successful application of AiFC probes in HeLa cells, we further inspected the performance of AiFC probes in human umbilical mesenchymal stem cells (HuMSC). Fluorescence signals of three individual pairs of AiFC probes were comparable to that in HeLa cells. These results demonstrated that AiFC probes were suitable for imaging different endogenous mRNAs in both epithelial cells and stem cells (Figure. 2b).

We then developed genetically encoded AiFC probes for detecting endogenous mRNAs. We first designed a system for high-level expression of short Split-Broccoli probes only of 30-40 nucleotides (Figure. S7). Next, we constructed two plasmids each encoding single Split-Broccoli probe sequence. Equal amount of two plasmids were co-transfected into HeLa cells. 48 hours after transfection, cells were incubated with DFHBI-1T and observed using live cell imaging (Figure. 3a). Intense fluorescent signals surrounding the nucleus were observed in cells expressing both AiFC probes; whereas negligible signals were observed in un-transfected cells and cells expressing single split probe A or B (Figure. 3b). The increased fluorescence in cells was also confirmed by flow cytometry (Figure. 3c). Real time imaging of β-actin mRNA were also performed. Time-lapse images revealed that the mRNA granules were moving in a restricted area in the cytoplasm. (Figure S8 and Video S1). Furthermore, we demonstrated the generality of AiFC by engineering a new RNA aptamer iSpinach [13b] for live-cell imaging of β-actin mRNA (Figure. S9 & S10).

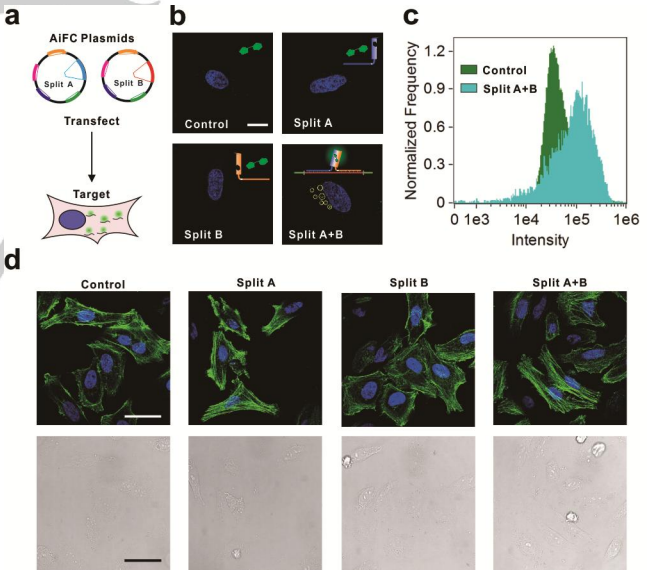

Figure 3. mRNA imaging with genetically encoded AiFC probes in living cells. (a) Scheme of the mRNA imaging principle by transfection of AiFC plasmids. (b) Confocal images of β-actin mRNA distribution in HeLa cells obtained via transfection of plasmids encoding AiFC probes. Nucleus is shown in blue (Hoechst). Scale bar: 20 μm. (c) Flow cytometry histogram of 10000 HeLa cells transfected with plasmids encoding Split-Broccoli AiFC probes (cyan) and control cells (green). (d) Cells transfected with AiFC plasmids targeting β-actin mRNA were stained for actin (green) and nuclei (blue), bright field images were shown in the lower panel. Scale bars: 50 μm.

Since the discovery of "GFP-mimicking" RNAs, Spinach and its derivatives have been widely utilized in the construction of

intracellular fluorescent sensors for various metabolites.[14b, 15] However, live-cell imaging based on this aptamer-fluorophore system was largely limited to abundant non-coding RNAs (eg 5S rRNA, 7L rRNA).[5, 7] Direct mRNA imaging remains challenging due to constraints including low brightness, impaired thermal stability and poor performance in the cytosolic K^+ and Mg^{2+} concentrations.[7b] For example, a recent example of mRNA imaging in bacteria relied on fusion of up to 64 copies of Spinach repeats to the 3' of a RFP mRNA that were expressed through IPTG induction, which significantly alters with their natural expression patterns.[16] In the present study, we have designed a novel AiFC strategy that circumvents direct modification of mRNA by introducing a pair of complementary probes. Resembling the GFP-based BiFC method, the split strategy greatly reduced background signals. We have thus demonstrated that this AiFC method is universal and applicable to RNA targets in various types of mammalian cell.

AiFC imaging minimally disturbs the natural behavior of mRNAs. We did not observe any effects on cell morphology or expression of actin upon transfection of AiFC probes (Figure. 3d & Figure S11). Since both probes are genetically encoded in plasmids for cellular expression, obviating invasive delivery of probes. Nevertheless, direct imaging of low-copy-number mRNAs remains a challenge due to the relatively low brightness of fluorescent RNA aptamers (as compared to GFP) in the cytosolic environment. For the moment, we have demonstrated the application of AiFC for qualitative observation of mRNAs in live cells. It remains challenging to quantify the exact amount of mRNAs via AiFC imaging only. The rapid advances in aptamer development and in-vitro selection have shown high potential for evolving high-brightness aptamers.[17] Since AiFC is a generic engineering method for DFHBI-binding fluorogenic RNA aptamers, we expect that, with further optimized aptamers, AiFC will provide a set of powerful tools for quantitative observation and real-time imaging of unmodified mRNA transcripts in mammalian cells.

In this contribution, we conclusively demonstrated the practical utility of novel live imaging technology uniquely tailored for real-time in vivo visualization experiments of RNA molecules in individual human cells. Significantly, cells imaged using our tools tolerated very well the required genetic engineering and imaging manipulations without manifestations of detectable changes in cells' viability and biological properties.

We observed that design of targeting sequence pairs does not require the immediate continuity of complementary sequences on targeted RNA molecules and some spatial distances are tolerated well. Therefore, it should be possible to extend the potential applications of this technology to the in vivo visualization analysis of RNA/RNA interactions of functional and regulatory significance, including spatio-temporal dynamics mRNA/microRNA [18] and microRNA/non-coding RNA-sponge binding events [19] in individual cells. Furthermore, it is technically feasible to engineer pairs of targeting aptamers in a single imaging construct to reliably discriminate and specifically bind defined region of RNA, DNA, and/or protein molecules. Thus, we envision the rapid expansion of novel applications and practical utility of the reported herein technology to the broad spectrum of biological and biomedical fields benefiting from in vivo single-cell visualization and mechanistic analysis of macromolecular interactions, including real-time biodynamics of formation and function of RNA/DNA, RNA/protein, and DNA/protein complexes.

Acknowledgements

This work was supported by National Natural Science Foundation of China (21390414, 31470970, 21227804, 21329501, 21675167, 31371493, 31571498), The National Basic Research Program of China (2013CB932803, 2013CB933802), National Key R&D Program of China (2016YFA0201200, 2016YFA0400900), the Youth Innovation Promotion Association from Chinese Academy of Sciences (2015211), and the Key Research Program of Frontier Sciences, CAS (QYZDJ-SSW-SLH031, QYZDJ-SSW-SLH019).

Keywords: Aptamer • fluorescence imaging • split aptamer • RNA imaging

[1] a) K. H. Chen, A. N. Boettiger, J. R. Moffitt, S. Wang, X. Zhuang, *Science* **2015**, *348*, aaa6090; b) T. Morisaki, K. Lyon, K. F. DeLuca, J. G. DeLuca, B. P. English, Z. J. Zhang, L. D. Lavis, J. B. Grimm, S. Viswanathan, L. L. Looger, T. Lionnet, T. J. Stasevich, *Science* **2016**, *352*, 1425-1429; c) C. Wang, B. Han, R. Zhou, X. Zhuang, *Cell* **2016**, *165*, 990-1001.

[2] P. R. Langersafer, M. Levine, D. C. Ward, *Proc. Natl. Acad. Sci. U. S. A.* **1982**, *79*, 4381-4385.

[3] a) Y. Xia, R. Zhang, Z. Wang, J. Tian, X. Chen, *Chem. Soc. Rev.* **2017**, *46*, 2824-2843; b) K. Y. Han, B. J. Leslie, J. Fei, J. Zhang, T. Ha, *J. Am. Chem. Soc.* **2013**, *135*, 19033-19038.

[4] a) E. Bertrand, P. Chartrand, M. Schaefer, S. M. Shenoy, R. H. Singer, R. M. Long, *Mol. Cell.* **1998**, *2*, 437-445; b) Y. Shav-Tal, X. Darzacq, S. M. Shenoy, D. Fusco, S. M. Janicki, D. L. Spector, R. H. Singer, *Science* **2004**, *304*, 1797-1800.

[5] J. S. Paige, K. Y. Wu, S. R. Jaffrey, *Science* **2011**, *333*, 642-646.

[6] W. Song, R. L. Strack, N. Svensen, S. R. Jaffrey, *J. Am. Chem. Soc.* **2014**, *136*, 1198-1201.

[7] a) R. L. Strack, M. D. Disney, S. R. Jaffrey, *Nat. Methods* **2013**, *10*, 1219-1224; b) G. S. Filonov, J. D. Moon, N. Svensen, S. R. Jaffrey, *J. Am. Chem. Soc.* **2014**, *136*, 16299-16308.

[8] A. K. Rath, A. Rentmeister, *Curr. Opin. Biotechnol.* **2015**, *31*, 42-49.

[9] a) C. Wu, S. Cansiz, L. Zhang, I. T. Teng, L. Qiu, J. Li, Y. Liu, C. Zhou, R. Hu, T. Zhang, C. Cui, L. Cui, W. Tan, *J. Am. Chem. Soc.* **2015**, *137*, 4900-4903; b) C. Y. Tay, L. Yuan, D. T. Leong, *ACS Nano* **2015**, *9*, 5609-5617; c) P. J. Santangelo, A. W. Lifland, P. Curt, Y. Sasaki, G. J. Bassell, M. E. Lindquist, J. E. Crowe, Jr., *Nat. Methods* **2009**, *6*, 347-349.

[10] a) Z. Wu, G. Q. Liu, X. L. Yang, J. H. Jiang, *J. Am. Chem. Soc.* **2015**, *137*, 6829-6836; b) L. He, D. Q. Lu, H. Liang, S. Xie, C. Luo, M. Hu, L. Xu, X. Zhang, W. Tan, *ACS Nano* **2017**, *11*, 4060-4066; c) S. Song, Z. Liang, J. Zhang, L. Wang, G. Li, C. Fan, *Angew. Chem.* **2009**, *121*, 8826-8830; *Angew. Chem. Int. Ed.* **2009**, *48*, 8670-8674; d) H. Xu, Q. Li, L. Wang, Y. He, J. Shi, B. Tang, C. Fan, *Chem. Soc. Rev.* **2014**, *43*, 2650-2661; e) D. Ye, X. Zuo, C. Fan, *Prog. Chem.* **2017**, *29*, 36-46.

[11] a) Y. Yang, J. Huang, X. Yang, K. Quan, H. Wang, L. Ying, N. Xie, M. Ou, K. Wang, *J. Am. Chem. Soc.* **2015**, *137*, 8340-8343; b) A. E. Prigodich, D. S. Seferos, M. D. Massich, D. A. Giljohann, B. C. Lane, C. A. Mirkin, *ACS Nano* **2009**, *3*, 2147-2152.

[12] a) T. K. Kerppola, *Annu. Rev. Biophys.* **2008**, *37*, 465-487; b) T. K. Kerppola, *Method Cell Biol.* **2008**, *85*, 431-470.

[13] a) G. S. Filonov, C. W. Kam, W. Song, S. R. Jaffrey, *Chem. Biol* **2015**, *22*, 649-660; b) A. Autour, E. Westhof, M. Ryckelynck, *Nucleic Acids Res.* **2016**, *44*, 2491-2500; c) K. D. Warner, M. C. Chen, W. Song, R. L. Strack, A. Thorn, S. R. Jaffrey, A. R. Ferre-D'Amare, *Nat. Struct. Mol. Biol* **2014**, *21*, 658-663.

[14] a) T. A. Rogers, G. E. Andrews, L. Jaeger, W. W. Grabow, *ACS Synth. Biol.* **2015**, *4*, 162-166; b) R. L. Strack, W. J. Song, S. R. Jaffrey, *Nat. Protoc.* **2014**, *9*, 146-155.

[15] a) C. A. Kellenberger, C. Chen, A. T. Whiteley, D. A. Portnoy, M. C. Hammond, *J. Am. Chem. Soc.* **2015**, *137*, 6432-6435; b) J. S. Paige, T. Nguyen-Duc, W. J. Song, S. R. Jaffrey, *Science* **2012**, *335*, 1194-1194; c) M. You, J. L. Litke, S. R. Jaffrey, *Proc. Natl. Acad. Sci. U. S. A.* **2015**, *112*, E2756-2765.

[16] J. Zhang, J. Fei, B. J. Leslie, K. Y. Han, T. E. Kuhlman, T. Ha, *Sci. Rep* **2015**, *5*, 17295-17303.

[17] a) H. K. Walter, J. Bauer, J. Steinmeyer, A. Kuzuya, C. M. Niemeyer, H. A. Wagenknecht, *Nano Lett.* **2017**, *17*, 2467-2472; b) I. Willner, M. Zayats, *Angew. Chem., Int. Ed.* **2007**, *46*, 6408-6418; c) A. D. Keefe, S. Pai, A. Ellington, *Nat. Rev. Drug Discovery* **2010**, *9*, 537-550; d) P. J. J. Huang, R. Kempaiah, J. W. Liu, *J. Mater. Chem.* **2011**, *21*, 8991-8993; e) H. Xing, L. Tang, X. Yang, K. Hwang, W. Wang, Q. Yin, N. Y. Wong, L. W. Dobrucki, N. Yasui, J. A. Katzenellenbogen, W. G. Helferich, J. Cheng, Y. Lu, *J. Mater. Chem. B* **2013**, *1*, 5288-5297.

[18] a) D. Baek, J. Villen, C. Shin, F. D. Camargo, S. P. Gygi, D. P. Bartel, *Nature* **2008**, *455*, 64-71; b) J. R. Lytle, T. A. Yario, J. A. Steitz, *Proc. Natl. Acad. Sci. U. S. A.* **2007**, *104*, 9667-9672.

[19] a) Q. Zheng, C. Bao, W. Guo, S. Li, J. Chen, B. Chen, Y. Luo, D. Lyu, Y. Li, G. Shi, L. Liang, J. Gu, X. He, S. Huang, *Nat. Commun.* **2016**, *7*, 11215; b) M. S. Ebert, J. R. Neilson, P. A. Sharp, *Nat. Methods* **2007**, *4*, 721-726.

10.1002/ange.201707795

WILEY-VCH

Entry for the Table of Contents

Layout 1:

COMMUNICATION

An aptamer-initiated fluorescence complementation (AiFC) method was developed for RNA imaging by engineering a green fluorescence protein (GFP)-mimicking turn-on RNA aptamer into two split fragments that could tandemly bind to target mRNA. The use of AiFC enables non-invasive, high-contrast real-time imaging of endogenous RNA molecules in living mammalian cells.

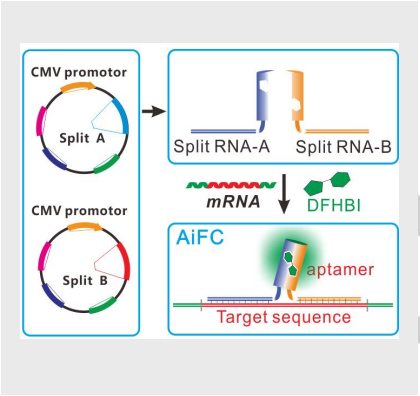

Zejun Wang, Yao Luo, Xiaodong Xie, Xingjie Hu, Haiyun Song, Yun Zhao, Jiye Shi, Lihua Wang, Gennadi Glinsky, Nan Chen, Ratnesh Lal, Chunhai Fan**

Page No. – Page No.

In-situ Spatial Complementation of Aptamer-mediated Recognition Enables Live-cell Imaging of Native RNA Transcripts in Real Time